Featured Original Research

Can cephalometric parameters be measured reproducibly using reduced-dose cone-beam computed tomography?

Check for updates

Michael N. Hoff [a,*], David Zamora [b], Charles Spiekerman [c], Johan K.M. Aps [d], Anne-Marie Bollen [e], Susan W. Herring [f], Fedora Katz [g]

[a] Assistant Professor, Department of Radiology, School of Medicine, University of Washington, Seattle, Washington
[b] Medical Physicist, Department of Radiology, School of Medicine, University of Washington, Seattle, Washington
[c] Research Scientist, Department of Biostatistics, School of Public Health, University of Washington, Seattle, Washington
[d] Associate Professor and Head of Dento-Maxillofacial Radiology, Oral Diagnostics and Surgical Sciences, UWA Dental School, University of Western Australia, Perth, WA, Australia
[e] Professor and Graduate Program Director, Department of Orthodontics, School of Dentistry, University of Washington, Seattle, Washington
[f] Professor, Departments of Orthodontics and Oral Health Sciences, School of Dentistry, University of Washington, Seattle, Washington
[g] Private practice, Marysville, Washington

ARTICLE INFO

ABSTRACT

Objective: To evaluate cone-beam computed tomography (CBCT) image quality via cephalometric measurement variability while reducing radiation exposure by altering the radiographic technique.
Materials and Methods: A human cadaver was imaged using a Morita Accuitomo 170 CBCT machine at various technique parameters: tube voltages of 60, 70, 80, and 90 kV, tube currents of 1, 2.5, and 5 mA, and rotational arcs of 180° and 360°. From the rotation data, standard cephalogram views were generated. Point radiation dose measurements were recorded at the entry of three key radiosensitive regions. Ten examiners measured seven cephalometric parameters on the conventional cephalogram and each derived view. Measurement error and dose were compared between radiographic techniques and a standard cephalometric procedure.
Results: Generally insignificant differences in measurement error were observed when rotation arc was reduced from 360° to 180°, when tube current was reduced from 5 mA to 2.5 mA, and when tube voltage was reduced from 90 kV to 80 kV and 70 kV. Radiation dose could be halved for either of the rotation arc or tube current reductions; reducing both yielded dose comparable to standard cephalometric imaging. Using 1 mA or 60 kV rendered nondiagnostic images.
Discussion: The study's cadaver included embalming fluid, a lack of patient-motion-induced image blur, and lesser bone density relative to a typical adolescent orthodontic patient, which can yield images not wholly representative of live patients.
Conclusion: Orthodontists could image with CBCT using a 180° arc of rotation, 2.5 mA, and 70 or 80 kV to reduce radiation dose while yielding images of adequate quality that are derived from three-dimensional data.

© 2019 World Federation of Orthodontists.

1. Introduction

Cone-beam computed tomography (CBCT) imaging is becoming an increasingly common tool for orthodontic diagnosis and treatment planning. It provides a lateral, third dimension (3D) that permits visualization of complex structures [1], which can be a convoluted task when acquiring multiple radiographic projections.

Tomographic procedures such as CBCT typically have a higher radiation dose than two-dimensional (2D) radiography, which historically has resulted in the avoidance of CBCT in the

predominately adolescent orthodontic population. Although standard clinical CBCT doses are not high enough to cause deterministic effects such as patient erythema or epilation, any amount of radiation is assumed to have a probability of causing stochastic effects (carcinogenesis), whereby increased dose results in higher cancer induction probability [2]. There is an even greater probability that stochastic effects may express in children, due to their longer expected life span and higher risk of DNA mutagenesis caused by more rapidly dividing cells [3]. The European Commission and the American Association of Oral and Maxillofacial Radiology have thus made clinical recommendations specifying that routine CBCT examinations are not indicated for the orthodontic patient [4,5].

The CBCT radiation dose detriment is often eclipsed by its 3D image reconstruction and reformat benefits. These benefits have led to CBCT being indicated for impacted teeth, cleft palate, and surgical interventions, and warrants an investigation into CBCT optimization to decrease radiation dose while maintaining diagnostic image quality [4,6]. Moderating the tube current (in milliamperes, mA) or exposure time (in seconds) can reduce the quantity of photons emitted by the x-ray tube; this reduces radiation exposure at the expense of reduced image contrast due to an associated relative increase in image noise. Reducing the arc of the CBCT tube rotation (in degrees) from 360° to 180° reduces exposure time and radiation dose by approximately 50%, at the expense of decreased 3D image fidelity and increased image graininess [7]. The tube voltage (in kilovolts, kV) determines the quality of the photons; decreasing it drops the average x-ray photon energy and penetrability in tissue, but typically this also decreases radiation exposure and increases image contrast. The aforementioned parameters may be appropriately reduced from adult settings when imaging smaller/younger patients to further reduce dose while retaining sufficient image quality [8].

The main objective of this study was to investigate how modifying CBCT tube current, tube voltage, and rotation arc affect image quality, with an eye for determining settings that reduce radiation dose while generating images that retain cephalometric/orthodontic diagnostic capacity. The reproducibility of cephalometric measurements (taken as a surrogate for image quality) performed on a standard cephalogram and CBCT-derived cephalograms acquired at manufacturer-recommended settings are compared with measurements on CBCT-derived cephalograms acquired with reduced tube voltages, currents, and rotation arc. The radiation dose was also recorded for each technique to ensure that all aspects of technique modification are considered. This proof-of-concept study shows that CBCT radiation dose may be decreased without impairing orthodontic assessment.

2. Material and methods

This study was approved by the local institutional review board (#49649). An embalmed male cadaver was sectioned horizontally mid-sternum to enable scanning of the oral cavity. The selection criteria were to have maximal teeth present for the provision of dental landmarks, minimal prosthetic work to avoid scanning artifacts, and a lack of fractures, asymmetries, or large deviations from normal anatomy. Maintenance of consistent cadaver positioning during scanning was enabled via injection of fixative.

Optically stimulated luminescence (OSL NanoDot, Landauer, IL) dosimeters, sensitive to doses as low as 50 μGy, were placed on anatomic regions that are relatively radiosensitive in live patients: the right eyelid, the right parotid area, and anterior to the thyroid gland. Dosimeters were replaced for each new acquisition, and three unexposed dosimeters were used as controls.

The cranial base, maxilla, and most of the mandible of the cadaver (cadaver preservation and the CBCT field of view [FOV] did not permit full mandibular scanning) were scanned 24 times using a clinical CBCT machine (3D Accuitomo 170; J. Morita MFG. Corp, Tokyo, Japan) at 0.25 mm isotropic resolution, 170x120-mm FOV, and at varied tube current (1, 2.5, or 5 mA), tube voltage (60, 70, 80, or 90 kV), and rotation arc (360°/17.5 s or 180°/9 s). The 180° arc consists of a half-rotation of the gantry, with x-rays emitted from the right side to the left side of the patient via the back of the head. Standardized Volume Computed Tomography Dose Index (CTDI$_{vol}$) values were recorded from the CBCT display for each technique. Manufacturer-recommended settings were represented by the 5 mA, 90 kV, and 360° combination. A 2D cephalogram and panoramic x-ray (Promax Dimax 4; Planmeca, Roselle, IL) was also acquired at standard manufacturer's settings (70 kV, 6 mA) with the cadaver's left side oriented toward the radiographic tube. Following scanning, OSL dosimeters were sent to their manufacturer (Landauer, Glenwood, IL) for dose calculations.

An image reconstruction system (Dolphin 3D, Chatsworth, CA) was used to generate a 2D cephalometric image from each of the 24 standardized 3D volumes (Fig. 1). The right Frankfort plane was horizontally oriented via sagittal-view assessment, the line passing between right and left Porion was horizontally oriented via frontal-view assessment, and the mid-sagittal plane was vertically oriented via axial-view assessment. All cephalometric images were de-identified of exposure parameters before interpretation to avoid examiner bias.

Following an instruction session, seven graduate students and three faculty in orthodontics examined randomly ordered parameter-blinded (exposure parameters were not shown on the images) cephalograms. Two days separated each image examination to prevent examiner fatigue and landmark recognition. Each examiner identified the following anatomical landmarks on each
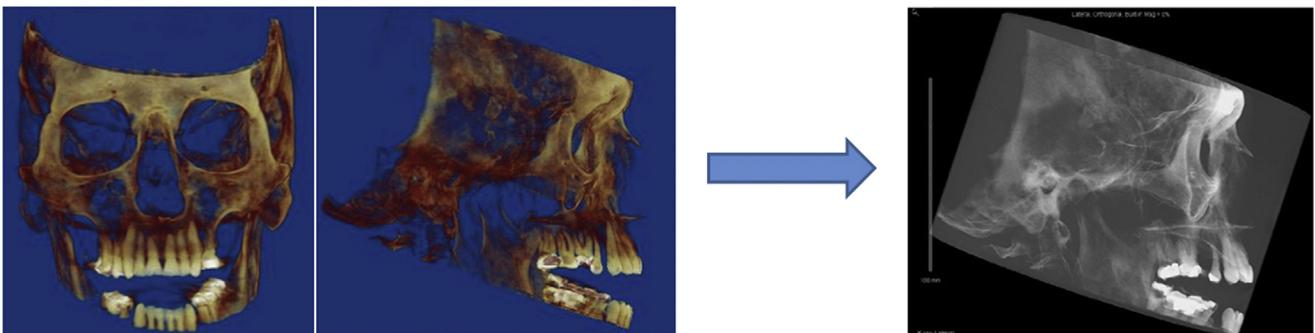

Fig. 1. Reoriented CBCT volume (left) and extracted cephalogram (right).
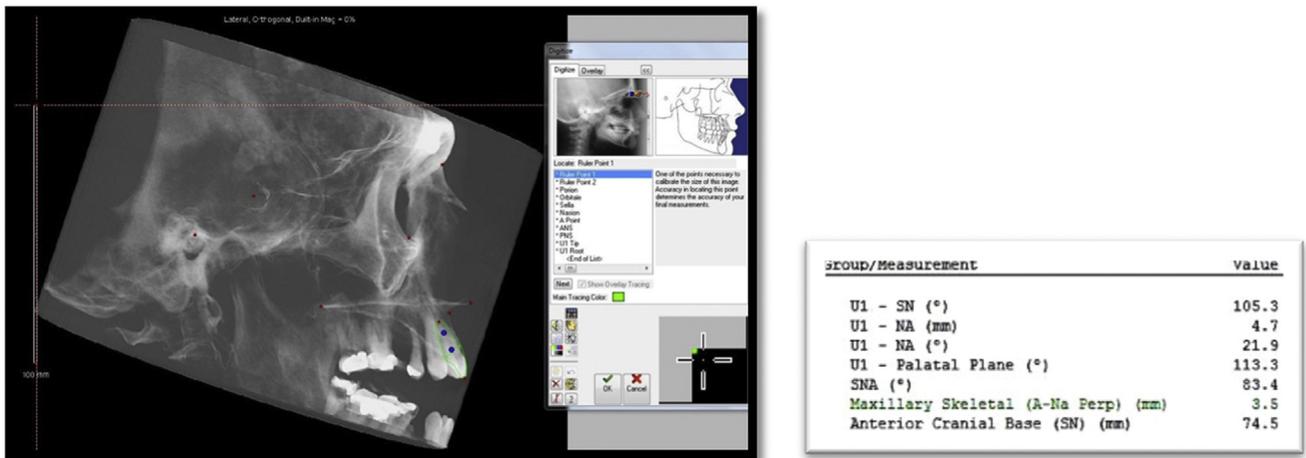
Fig. 2. Anatomical landmark identification and automated cephalometric measurement on a cephalogram using Dolphin.

image: Sella, Nasion, Porion, Orbitale, anterior nasal spine (ANS), posterior nasal spine (PNS), the deepest point along the maxilla's outline curve (A-Point), and maxillary central incisor (U1) incisal and root tips. Observers calibrated images via landmarks on a 100-mm digital ruler, used the same computers and lighting conditions, and were permitted to use image windowing and leveling. Double measurements were obtained by duplicating four techniques (90 kV/5 mA/360°, 90 kV/2.5 mA/360°, 90 kV/2.5 mA/180°, 60 kV/ 1 mA/360°) and randomly inserted the additional images among the others to assess intraexaminer reliability.

Figure 2 depicts how the following automated skeletal and dental measurements were extracted: SNA angle (Sella-Nasion-A-point angle, degrees), A-N perpendicular (A-point to perpendicular line through N-point distance, mm), U1-NA (maxillary incisoid Nasion labial surface to A-point line distance, mm, and angle, degrees), U1-SN (maxillary incisor axis to S-N line angle, degrees), and U1-PP (maxillary incisor axis to palatal plane angle, degrees).

Image quality was assessed via the mean absolute deviation of the 10 observer measurements from the corresponding mean for each cephalometric variable. Measurement errors were compared via a paired permutation-test: differences between errors at varied settings were tested for significance from zero (null-hypothesis) over 10,000 Monte-Carlo permutations [9]. Interobserver error among raters was calculated in the same fashion, whereas

Table 1

Mean absolute deviations (error) from cephalometric measurement means across the 10 examiners, CTDIvol values, and point-doses from parotid and eyelid dosimeters for each radiographic technique, including the cephalogram and panoramic at the bottom in gray

Technique			Mean absolute deviation (error)							Dose metrics (mGy)		
Rotation/time	mA	kV	A-Nperp (mm)	S-N (mm)	U1-NA (mm)	SNA (°)	U1-NA (°)	U1-PP (°)	U1- SN (°)	CTDIvol	Eyelid - point	Parotid - point
360°/17.5s	5	60	0.60	0.39	0.47	0.39	1.49	1.27	1.33	2.92	2.31	2.23
		70	0.51	0.48	0.38	0.31	1.17	1.30	1.20	4.47	3.59	3.24
		80	0.50	0.33	0.50	0.52	1.27	1.18	1.35	6.38	4.77	4.53
		90	0.67	0.26	0.37	0.48	1.50	1.43	1.60	8.73	6.39	5.70
	2.5	60	0.81	0.41	0.66	0.46	1.83	1.71	1.62	1.52	1.20	1.16
		70	0.70	0.35	0.71	0.34	1.79	1.61	1.54	2.30	1.84	1.66
		80	0.79	0.30	0.51	0.42	1.15	0.98	1.14	3.28	2.35	2.27
		90	0.87	0.27	0.38	0.38	1.22	1.17	1.11	4.48	3.33	2.88
	1	60	1.46	1.17	0.94	0.94	3.00	2.87	2.81	0.66	0.49	0.51
		70	2.18	3.29	0.98	2.26	2.06	2.10	2.40	0.99	0.82	0.71
		80	1.22	0.19	0.61	0.60	1.58	1.43	1.38	1.41	1.04	0.92
		90	0.96	0.32	0.78	0.42	1.52	1.27	1.43	1.93	1.39	1.23
180°/9s	5	60	0.83	0.50	0.30	0.46	1.52	1.36	1.29	1.52	0.22	1.16
		70	1.00	0.41	0.39	0.27	0.81	0.62	1.00	2.29	0.40	1.62
		80	0.44	0.45	0.34	0.31	1.35	1.20	1.47	3.27	0.59	2.23
		90	0.56	0.27	0.42	0.38	1.15	1.26	1.34	4.47	0.88	2.80
	2.5	60	1.10	0.84	0.86	0.55	2.12	2.03	1.94	0.78	0.13	0.61
		70	1.17	0.26	0.52	0.38	2.11	1.78	1.84	1.18	0.22	0.89
		80	0.45	0.41	0.51	0.28	1.90	1.73	1.88	1.68	0.34	1.12
		90	0.72	0.38	0.65	0.41	1.83	1.49	1.68	2.30	0.41	1.51
	1	60	2.02	0.85	2.23	1.57	2.92	1.70	1.76	0.34	0.06	0.25
		70	1.27	0.59	1.41	0.86	1.33	1.01	0.80	0.51	0.09	0.34
		80	0.96	0.34	1.18	0.96	1.60	1.11	1.17	0.72	0.14	0.53
		90	1.04	0.28	0.56	0.54	1.20	0.98	1.25	0.99	0.20	0.65
Cephalogram			3.08	0.58	1.28	1.29	2.20	2.11	1.92	N/A	0.1 (1.1 with panoramic)	

A-N perp, A-point to perpendicular line through N-point distance; NA, Nasion labial surface to A-point line distance; PP, palatal plane; SN, sella nasion; SNA, SN A point; U1, maxillary central incisor.

Thyroid dosimeters were not included due to underexposure. For interrater reliability, radiographic techniques 360°−1 mA-60 kV, 360°−2.5 mA-90 kV, 360°−5 mA-90 kV, and 180°−2.5 mA-90 kV were duplicated and their measures averaged.

intraobserver error was analyzed using Dahlberg's formula on the double measurements. Statistical data were analyzed with the R language and environment for statistical computing [10], and dosimetry data were analyzed using Medcalc statistical software version 17.4 (Medcalc Software, Ostend, Belgium, 2017, http://www.medcalc.org).

3. Results

Radiographic techniques and their corresponding mean absolute measurement deviations, CTDI$_{vol}$ values, and point dose measurements are presented in Table 1. Note that CTDI$_{vol}$ values indicate radiation output and thus offer a useful index for tracking the radiographic technique. Also note that the 360°, 1-mA, 70-kV image had a high relative mean absolute deviation; its image quality was substandard due to machine malfunction, and therefore the corresponding measurement data were removed from further statistical analyses.

Measurement errors generally increased as tube currents decreased. Figure 3 depicts images acquired at 90 kV, 360° rotation, and (Fig. 3A) 5-mA (manufacturer-recommended settings), (Fig. 3B) 2.5 mA, and (Fig. 3C) 1 mA that become respectively grainier. Figure 4 depicts point measurements plotted vertically, with varied radiological technique separated horizontally and indicated by point shape and color. Most of the plots exhibit higher measurement variability as tube current decreases at a given tube voltage and rotation arc. Table 2 shows mean errors of each cephalometric measurement over all rotation arcs and tube voltages for each tube current, and indications of statistically significant ($P < 0.05$) differences between the mean errors. All measurements except the U1-PP and U1-SN angle measurements tend to vary more with reduced tube current.

Decreasing tube voltage subtly increased (although not always significantly) measurement variability. Figure 3 shows images acquired at 5 mA and 360° rotation arc with varied tube voltage; whereas image quality was similar at (Fig. 3A) 90 kV (manufacturer-recommended setting) and (Fig. 3D) 80 kV, it degenerated slightly at (Fig. 3E) 70 kV and (Fig. 3F) 60 kV. Figure 4 validates that for a given milliampere and rotation arc, there is a general trend of greater cephalometric measurement variability as voltage is decreased. Table 2 also includes mean errors for each kV over all rotation arcs and mA with statistical significance information. There is almost always a significant increase in measurement variability for 60-kV measurements relative to higher tube voltages. There is rarely a significant change in measurement variability among 70, 80, or 90 kV.

Figure 3 also compares images acquired using 5 mA and 90 kV with a rotation arc of (Fig. 3A) 360° (manufacturer-recommended setting), and (Fig. 3G) 180°; the latter technique yielded a slightly grainier image. The corresponding mean errors across all milliamperes and kilovolts for each rotation arc and their permutation-test-determined P values are detailed in Table 3. Aside from significant ($P < 0.05$) increases in mean measurement error for A-N perp and U1-NA length measurements, there was no significant change in error when the rotation arc was reduced from 360° to 180°.

Scrutiny of Figure 4 reveals that measurement error generally increased at 1 mA, moderately increased at 60 kV, and was similar for the rotation arcs. The gray-colored traditional cephalogram measurements show high relative variability, with the exception of the SN length measurement.

Table 4 details resident and faculty mean measurement errors, their differences, and the significance of these differences. Overall insignificant ($P > 0.05$) differences indicated similar measurement reliability for faculty and residents. An intraexaminer reliability analysis (Table 5) revealed that examiner reliability depended on image quality and measurement type rather than examination reproducibility. Higher-quality images and less error-prone measurements like SN (mm), SNA (°), U1-PP (°) had the highest examiner reliability, whereas lower-quality images and more error-prone measurements like A-N perp (mm) and U1-NA (mm) had lower reliability.

Figure 5 depicts dosimeter-location-specific box and whisker plots of radiation point dose values stratified by (Fig. 5A) milliamperes, (Fig. 5B) kilovolts, and (Fig. 5C) rotation arc. Measured radiation dose for eyelid and parotid gland dosimeters increased with milliamperes, kilovolts, and rotation arc. Sensors for the traditional cephalogram captured 0.1 mGy cumulative point dose, whereas the associated panoramic x-ray yielded 1.0 mGy cumulative point dose.

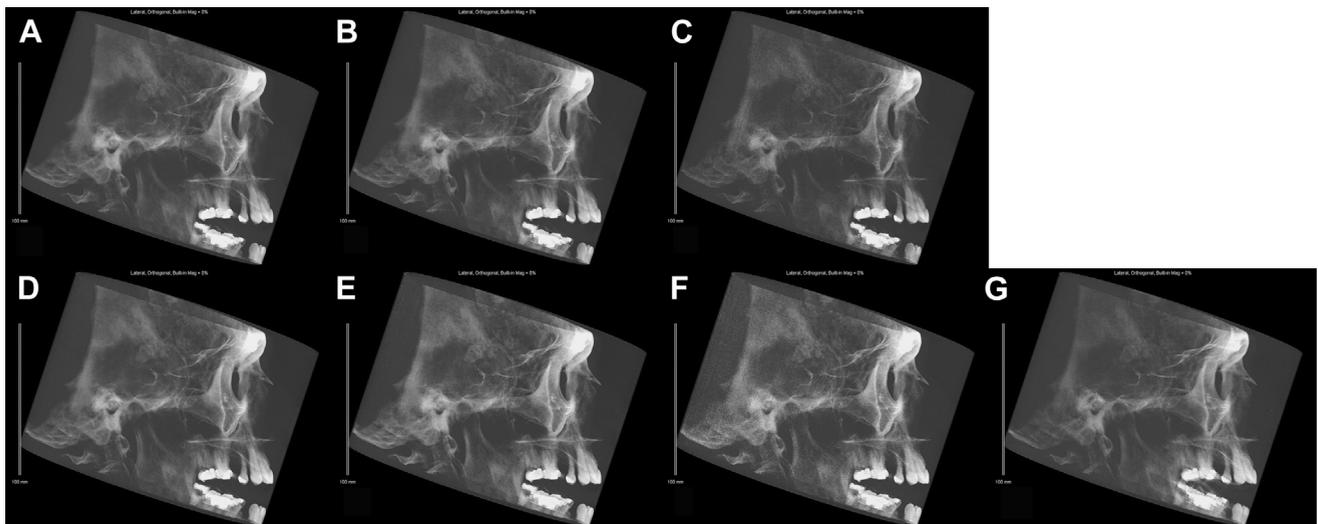**Fig. 3.** Images taken using (A) 90 kV, 5 mA, and 360° rotation arc; (B) 90 kV, 2.5 mA, and 360° arc; (C) 90 kV, 1 mA, and 360° arc; (D) 80 kV, 5 mA, and 360° arc; (E) 70 kV, 5 mA, and 360° arc; (F) 60 kV, 5 mA, and 360° arc; and (G) 90 kV, 5 mA, and 180° arc. Images taken using 5 mA and 360° rotation arc, with (A) 90 kV, (B) 80 kV, (C) 70 kV, and (D) 60 kV. Images taken using 5 mA and 90 kV, with (A) 360° and (B) 180°.
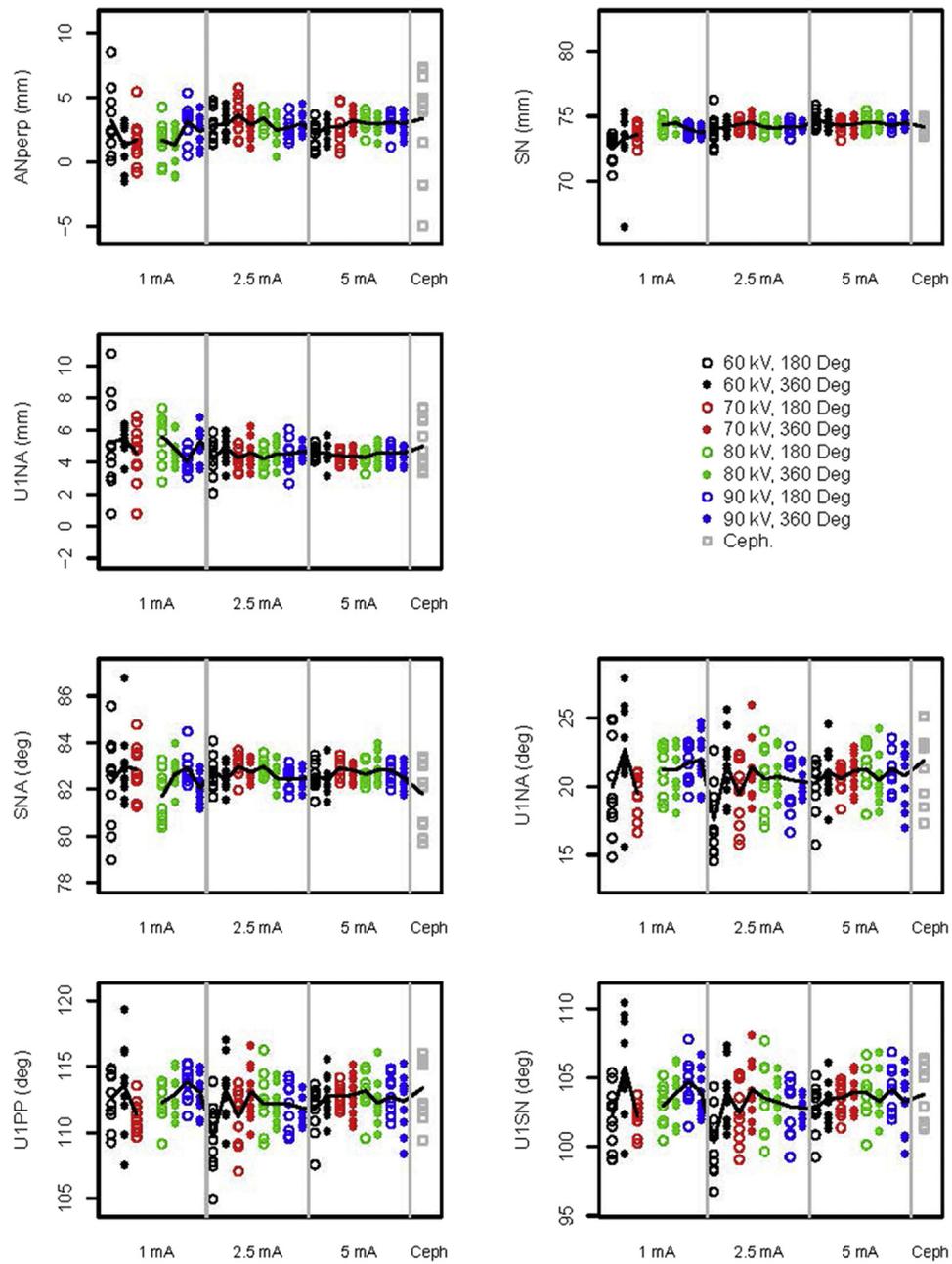
Fig. 4. Cephalometric measurement distribution for A-Nperp (mm), SN (mm), U1-NA (mm), SNA (°), U1-NA (°), U1-PP (°), and U1-SN (°) on separate plots. Measurements from varied radiographic techniques are plotted vertically with dots and are delimited horizontally for milliamperes, by color for kilovolts, and hollow or filled for rotation arc. Gray squares indicate measurements on the standard cephalogram. Black lines connect each technique's measurement mean. Greater point spread for a given technique indicates greater mean absolute measurement deviation and larger disagreement between examiners.

4. Discussion

The objective of this study was to assess the relationship among CBCT technique, image quality, and radiation output. This was achieved by varying CBCT tube current, tube voltage, and arc of rotation and measuring cephalometric parameters on lateral CBCT-derived cadaverous cephalograms while collecting radiation dose. Some lower-dose CBCT techniques not only yielded inherently 3D datasets, but comparisons with the standard cephalogram indicated that they also maintain image quality that is suitable for cephalometric purposes.

Although cephalometric measurement error can serve as a powerful metric to quantify image quality, some factors must be considered before error analysis. Error variation does not always ascertain the diagnostic capacity of an image. Increased error may still be comparable with standard cephalogram error, indicating acceptable image quality. On the other hand, some procedures such as fenestration assessment, crestal bone level measurement, periodontal ligament space visualization, and dental root resorptive defect identification require images of such high resolution that decreased measurement error may still be insufficient for orthodontic diagnosis. It is thus essential that the specific diagnostic task is considered before CBCT technique selection to avoid unnecessary repeat exposures caused by inadequate image quality. The FOV and spatial resolution also play an important role [11], and should be optimized for a given patient, procedure, desired image quality, and

Table 2
Mean absolute deviations (error) across all 10 examiner measurements for each mA setting over all kV and rotational arc variations, and for each kV setting over all mA and rotational arc variations

	A-Nperp (mm)	*Significantly different from	SN (mm)	*Significantly different from	U1-NA (mm)	*Significantly different from	U1-NA (deg)	*Significantly different from	SNA (deg)	*Significantly different from	U1-PP (deg)	*Significantly different from	U1-SN (deg)	*Significantly different from
						Mean absolute deviation (error) and significance from permutation test								
1 mA	1.31	2.5, 5 mA	0.59	2.5, 5 mA	1.06	2.5, 5 mA	1.80	2.5, 5 mA	0.85	2.5, 5 mA	1.41	-	1.51	-
2.5 mA	0.78	1, 5 mA	0.38	1 mA	0.61	1 mA	1.70	1, 5 mA	0.39	1 mA	1.53	-	1.55	-
5 mA	0.63	1, 2.5 mA	0.39	1 mA	0.40	1 mA	1.33	1, 2.5 mA	0.38	1 mA	1.25	-	1.34	-
60 kV	1.17	80, 90 kV	0.76	70, 80, 90 kV	0.86	90 kV	2.05	90 kV	0.74	70, 80, 90 kV	1.74	70, 80, 90 kV	1.78	70 kV
70 kV	0.93	-	0.42	60, 90 kV	0.68	-	1.44	-	0.43	60 kV	1.27	60 kV	1.28	60 kV
80 kV	0.73	60 kV	0.34	60 kV	0.61	60 kV	1.47	60 kV	0.51	60 kV	1.27	60 kV	1.40	60 kV
90 kV	0.73	60 kV	0.28	60, 70 kV	0.54	60 kV	1.41	60 kV	0.42	60 kV	1.28	60 kV	1.38	-

A-N perp, A-point to perpendicular line through N-point distance; N-A, Nasion labial surface to A-point line distance; PP, palatal plane; SN, sella nasion; SNA, SN A point; U1, maxillary central incisor.
Statistically significant differences are indicated relative to each other setting value if *P< 0.05, where P values are derived via Monte-Carlo permutation tests.

Table 3
Mean absolute deviations (error) for both rotational arc settings across all ten examiner measurements of all mA and kV variations

Measurement	Mean error per rotation arc		*Significantly different? (P-value)
	180°	360°	
A-N perp (mm)	1.02	0.77	Yes (0.017)
S-N (mm)	13.16	13.00	No (0.95)
U1-NA (mm)	1.08	0.74	Yes (0.001)
U1-NA (deg)	3.86	3.75	No (0.58)
SNA (deg)	14.69	14.49	No (0.95)
U1-PP (deg)	20.02	19.96	No (0.99)
U1-SN (deg)	18.38	18.34	No (0.99)

A-N perp, A-point to perpendicular line through N-point distance; N-A, Nasion labial surface to A-point line distance; PP, palatal plane; SN, sella nasion; SNA, SN A point; U1, maxillary central incisor.
Statistical significance and P values given between settings (significant if *P < 0.05), derived via Monte-Carlo permutation tests.

radiation dose. Finally, the number of reviewers (and patients/cadavers) can affect the statistical power in the evaluation of any metric.

This study uniquely uses measurement error to assess cephalometric diagnostic capacity at variable CBCT technique to largely confirm the results from recent studies showing that dose reduction is possible without clinically relevant degradation of image quality [12]. Others have used questionnaires [11], lesion-size measurements [13], and image quality calculations on phantoms [14,15] to not only determine that increased milliampere improves image quality, but also that lowered milliampere or kilovolt may retain diagnostic capacity at reduced dose. A reduction of CBCT rotation arc from 360° to 180° has also shown to permit diagnostic imaging [7,16—19]: one group found that cadaverous buccal bone height and thickness measurement error was similar or even reduced relative to a standard cephalogram at CBCT techniques as low as 2.5 mA, 70 kV, and 180° rotation, and that only high-resolution imaging warrants a 360° rotation arc [18]. Higher kilovolts, milliamperes, and rotation arc demonstrated marginal decreases in measurement error, whereas lower values like 1 mA and/or 60 kV showed increased error.

Radiation dose is a benchmark of patient detriment in radiological studies and was monitored to quantify the trade-off to increased image quality via radiological technique. This study measured increased radiation point dose that corresponded with increased radiographic technique, where $CTDI_{vol}$ provided an index to track increases in mA, kV, and rotation arc. When it is considered that a 1.0 mGy panoramic x-ray traditionally accompanies the

Table 4
Mean error over all radiographic techniques for each measurement, stratified by examiner type (residents and faculty)

Measurement	Mean error		Error differences	95% confidence interval		P Values (none *significant)
	Residents (n=7)	Faculty (n=3)				
U1-SN (deg)	1.82	1.46	0.36	−0.05	0.90	0.10
U1-NA (deg)	1.85	1.63	0.22	−0.27	0.81	0.35
U1-NA (mm)	0.83	0.64	0.19	−0.09	0.45	0.17
U1- PP (deg)	1.66	1.32	0.35	−0.23	1.02	0.17
SNA (deg)	0.67	0.55	0.12	−0.20	0.44	0.41
A-N perp (mm)	1.02	1.19	-0.17	−0.67	0.31	0.43
SN (mm)	0.69	0.61	0.08	−0.39	0.58	0.74

A-N perp, A-point to perpendicular line through N-point distance; N-A, Nasion labial surface to A-point line distance; PP, palatal plane; SN, sella nasion; SNA, SN A point; U1, maxillary central incisor.
Error differences, confidence intervals, and P values (none significant with *P < 0.05) are given to assess interexaminer reliability.

Table 5
Dahlberg's formula value and coefficient of variation by image type for the four duplicated images

Measurement	Dahlberg value (% of mean)				All 4 images combined
	90 kV/5 mA/360°	90 kV/2.5 mA/360°	60 kV/1 mA/360°	90 kV/2.5 mA/180°	
U1-SN (deg)	7.1 (7%)	4.1 (4%)	13 (13%)	5.8 (6%)	8.2 (8%)
U1-NA (deg)	5.7 (27%)	4.4 (21%)	13.5 (64%)	6.5 (31%)	8.3 (40%)
U1 NA (mm)	1.7 (36%)	2 (41%)	6 (125%)	3 (64%)	3.6 (75%)
U1-PP (deg)	6.5 (6%)	4.6 (4%)	11.3 (10%)	5.8 (5%)	7.5 (7%)
SNA (deg)	1.9 (2%)	2 (2%)	6.8 (8%)	2.1 (2%)	3.8 (5%)
A-N perp (mm)	1.4 (55%)	3.2 (122%)	3.7 (143%)	3.6 (138%)	3.1 (120%)
SN (mm)	1.2 (2%)	1.7 (2%)	9.3 (13%)	1 (1%)	4.8 (6%)

A-N perp, A-point to perpendicular line through N-point distance; N-A, Nasion labial surface to A-point line distance; PP, palatal plane; SN, sella nasion; SNA, SN A point; U1, maxillary central incisor.
Inconsistent % values for a given technique repetition indicate that interexaminer reliability depends more on image quality and measurement type than on overall examination reproducibility.
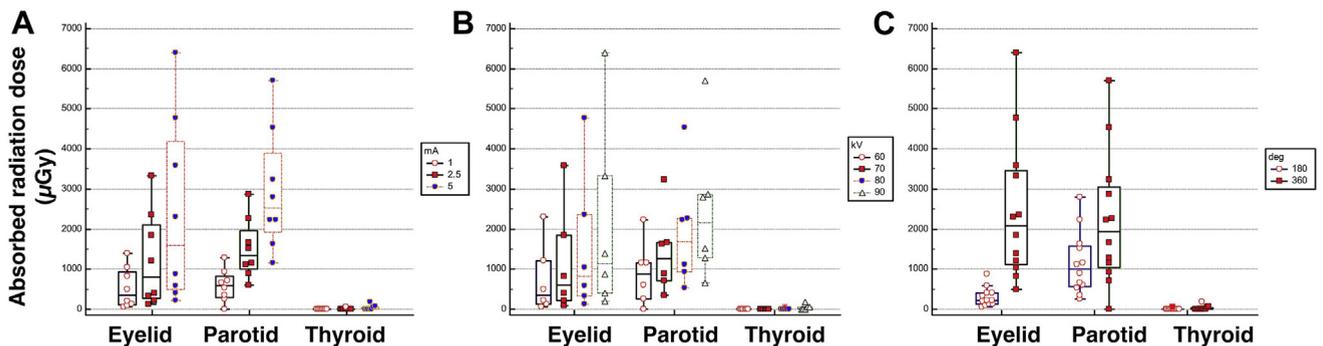

Fig. 5. Radiation dose measurements with box and whisker plots overlaid to indicate quartiles and median. Measurements are segregated horizontally and by color depending on dosimeter location and radiographic technique: (A) milliampere, (B) kilovolt, and (C) arc of rotation.

standard cephalometric acquisition, cumulative CBCT point doses were comparable at lower milliampere values and 180° rotation arc, with less measurement variability than the cephalogram at almost all settings (not including 60 kV−1 mA). A big advantage of using the 180° rotation arc was the lack of full eyelid exposure, because the limited arc only yields radiation emission to the back and sides of the head. This prevented direct exposure of the corresponding dosimeter, resulting in less radiation risk to this radiosensitive organ. All thyroid doses were minimal due to a similar lack of direct exposure. It should be noted that because the mandible was not fully imaged, the thyroid dose measurement was compromised; this is not a major issue given that the dose measures are compared relatively and not absolutely in this study.

There are some limitations to the application of this study directly to live patients due to the testing being executed on a single cadaver, scanner, and dosimeter set. Images acquired of a cadaver can yield image quality not representative of in vivo imaging, due to the effects of the embalming fluid on imaging, the lack of patient-motion-induced image blur, and the lesser bone density yet greater tissue to penetrate the large 82-year-old cadaver (relative to a typical adolescent orthodontic patient). This scenario is unavoidable, as it is unethical to scan live patients for testing purposes due to the deleterious effects of ionizing radiation, and it is difficult to obtain adolescent cadavers for experimentation. Testing the reproducibility of dose measurements via multiple dose calculations at the same physical locations was limited by the high cost of optically stimulated luminescence dosimeters, the need to mail them out for measurement tabulation, and the difficulty in exact dosimeter replacement. However, the relative dose estimates made are still of high value to qualify the safety sacrifice needed for radiographic technique alterations. Finally, only one scanner was tested in this study, and so it must be emphasized that protocol

optimization is necessary on any scanner before establishing clinical methods; the manufacturer's settings do not necessarily guarantee the highest or most suitable image quality for a given radiation dose. Despite these limitations, it is apparent that a low-dose radiographic technique does not necessarily preclude the ability to perform cephalometric measurements.

5. Future directions

Future studies will perform similar measurements using a larger FOV that covers the entire mandible, and on other cephalometric reconstructions such as maximum intensity projections and 3D volume-rendered images to evaluate how they are affected by the discussed dose reductions. This and future studies' findings draw attention to the potential for developing customized exposure protocols that decrease radiation dose while retaining image functionality.

6. Conclusions

The present study demonstrates the ability to sustain cephalometric image quality while reducing CBCT radiation dose through modifications to CBCT radiographic settings in a cadaver. Cephalometric images derived from CBCT scans that used current reduction from 5 mA to 2.5 mA or rotation arc reduction from 360° to 180° sustained diagnostic quality while halving the CBCT radiation dose. Lowering the voltage from 90 kV to 80 kV or even to 70 kV significantly reduced radiation dose without sacrificing the derived image's diagnostic value. Lowering the exposure settings to 1 mA and 60 kV for the Accuitomo 170 CBCT machine yielded images of poor diagnostic quality that are unreliable for cephalometric measurements.

References

[1] Moyers RE, Bookstein FL. The inappropriateness of conventional cephalometrics. Am J Orthod 1979;75:599—617.

[2] National Research Council. Health risks from exposure to low levels of ionizing radiation: BEIR VII Phase 2. Washington, DC: The National Academies Press; 2006.

[3] Theodorakou C, Walker A, Horner K, Pauwels R, Bogaerts R, Jacobs R. Estimation of paediatric organ and effective doses from dental cone beam CT using anthropomorphic phantoms. Br J Radiol 2012;85:153—60.

[4] The SEDENTEXCT project. Cone beam CT for dental and maxillofacial radiology (Evidence-Based Guidelines). Luxembourg: European Commission; 2011.

[5] American Academy of Oral and Maxillofacial Radiology. Clinical recommendations regarding use of cone beam computed tomography in orthodontics. [corrected]. Position statement by the American Academy of Oral and Maxillofacial Radiology. Oral Surg Oral Med Oral Pathol Oral Radiol 2013;116:238—57.

[6] Kapila SD, Nervina JM. CBCT in orthodontics: assessment of treatment outcomes and indications for its use. Dentomaxillofac Radiol 2015;44:20140282.

[7] Pauwels R, Zhang G, Theodorakou C, et al. Effective radiation dose and eye lens dose in dental cone beam CT: effect of field of view and angle of rotation. Br J Radiol 2014;87:20130654.

[8] U.S. Food and Drug Administration. Radiation-emitting products. 2018. Available at: https://www.fda.gov/radiation-emittingproducts/. [Accessed 27 February 2019].

[9] Dwass M. Modified randomization tests for nonparametric Hypotheses. Ann Math Statist 1957;28:181—7.

[10] R Core Team. R: A language and environment for statistical computing. Vienna, Austria: R Foundation for Statistical Computing; 2019. Available at: https://www.r-project.org/.

[11] Kwong JC, Palomo JM, Landers MA, Figueroa A, Hans MG. Image quality produced by different cone-beam computed tomography settings. Am J Orthod Dentofacial Orthop 2008;133:317—27.

[12] Goulston R, Davies J, Horner K, Murphy F. Dose optimization by altering the operating potential and tube current exposure time product in dental cone beam CT: a systematic review. Dentomaxillofac Radiol 2016;45:20150254.

[13] Gamache C, English JD, Salas-Lopez AM, Rong J, Akyalcin S. Assessment of image quality in maxillofacial cone-beam computed tomography imaging. Semin Orthod 2015;21:248—53.

[14] Xu J, Reh DD, Carey JP, Mahesh M, Siewerdsen JH. Technical assessment of a cone-beam CT scanner for otolaryngology imaging: image quality, dose, and technique protocols. Med Phys 2012;39:4932—42.

[15] Pauwels R, Silkosessak O, Jacobs R, Bogaerts R, Bosmans H, Panmekiate S. A pragmatic approach to determine the optimal kVp in cone beam CT: balancing contrast-to-noise ratio and radiation dose. Dentomaxillofac Radiol 2014;43:20140059.

[16] Lennon S, Patel S, Foschi F, Wilson R, Davies J, Mannocci F. Diagnostic accuracy of limited-volume cone-beam computed tomography in the detection of periapical bone loss: 360 degrees scans versus 180 degrees scans. Int Endod J 2011;44:1118—27.

[17] Durack C, Patel S, Davies J, Wilson R, Mannocci F. Diagnostic accuracy of small volume cone beam computed tomography and intraoral periapical radiography for the detection of simulated external inflammatory root resorption. Int Endod J 2011;44:136—47.

[18] Cook VC, Timock AM, Crowe JJ, Wang M, Covell Jr DA. Accuracy of alveolar bone measurements from cone beam computed tomography acquired using varying settings. Orthod Craniofac Res 2015;18:127—36.

[19] Pauwels R, Beinsberger J, Collaert B, et al. Effective dose range for dental cone beam computed tomography scanners. Eur J Radiol 2012;81:267—71.